

Soil-water characteristic curve and permeability coefficient prediction model for unsaturated loess considering freeze-thaw and dry-wet

Yaling Chou^{1#} , Lijie Wang¹ 

Article

Keywords

Unsaturated loess
Soil-water characteristic curve
Filter paper method
Permeability coefficient function
Freeze-thaw cycle
Dry-wet action

Abstract

The SWCC has played an important role in studying the physical-mechanical behavior and hydraulic property of unsaturated soils. Laboratory experiments of SWCC were performed on unsaturated loess based on filter paper method considering freeze-thaw cycle, coupling of freeze-thaw cycle and dry-wet action. The main results indicate that: (1) With the increase of freeze-thaw cycle or freeze-thaw and dry-wet coupling, the matric suction was logarithmically decreasing and the dry-wet path affected matric suction significantly. There were obvious hysteresis loops between the two SWCC curves of different dry-wet paths, which increased with the increase of water content. (2) The Gardner Model was more appropriate to describe the SWCC, and through measured SWCC from Gardner Model and Childs & Collis-George Model, the prediction model of unsaturated loess permeability coefficient was gained, which had an exponential relationship with matric suction and a power function relationship with volumetric water content, respectively. (3) The vertical distribution model of permeability coefficient under one-dimensional steady state flow was established. The vertical permeability coefficient gradually decreased from groundwater table to ground surface, it decreased first then increased and gradually stabilized with the increase of freeze-thaw cycle at the same depth of soil.

1. Introduction

The soil water characteristic curves (SWCCs) describe the relationship between soil water content (or saturation) and soil water potential (or suction), which is the basis to explain a variety of processes in unsaturated soils, ranging from transport phenomena to mechanical behaviors (Liu et al., 2012). Loess is widely distributed in northwestern China, and mainly concentrated in arid and semi-arid areas, belonging to unsaturated soil and seasonally frozen region. Therefore, the complex climatic environments including repeated freezing and thawing, evaporation and rainfall have a significant influence on the mechanical behavior of shallow unsaturated loess. And the physical and mechanical properties of shallow unsaturated loess have always been changing dynamically due to the disturbance of external climate. Especially, the roadbed, slope engineering, airport, water conservancy and other engineering projects are mostly in the shallow unsaturated zone, and are extensively exposed to the air. That is to say, most geotechnical projects are built in the unsaturated zone, which is located near the ground surface area forming the connection between weather systems above and saturated ground below, and interacts with the surrounding environment.

In the aspect of theoretical research, the scholars at home and abroad have made rich researches on SWCC, and a lot of useful conclusions were drawn (Bishop et al., 1960; Fredlund et al., 1994; Fredlund and Rahardjo, 1997). The SWCC reflecting the engineering mechanical properties and hydraulic property of unsaturated soil indicates the relationship between the matric suction and the volumetric water content of unsaturated soil, and is one of the constitutive relations explaining the mechanical properties of unsaturated soil. It is also of great significance for predicting and analyzing the hydraulic properties, shear strength and deformation characteristic of unsaturated soils, and is of important practical value for analyzing engineering problems such as slope stability evaluation and foundation deformation calculation (Chen, 1999; Wang et al., 2003; Xiong et al., 2005; Li et al., 2007; Lu and Cheng, 2007; Bai et al., 2011). Fredlund et al. (1994) established the permeability function of unsaturated soil by the SWCC. Vanapalli et al. (1996) and Fredlund et al. (1996) both studied the relationship between the SWCC and unsaturated soil strength. Sillers et al. (2001) systematically analyzed and evaluated various fitting models of SWCC. Liu et al. (2011) carried out a series of

[#]Correspondence author. E-mail address: chouyaling@lzb.ac.cn

¹Lanzhou University of Technology, Key Laboratory of Disaster Prevention and Mitigation in Civil Engineering, Lanzhou, China.

Submitted on October 13, 2020; Final Acceptance on December 30, 2020; Discussions open until May 31, 2021.

DOI: <https://doi.org/10.28927/SR.2021.058320>



This is an Open Access article distributed under the terms of the Creative Commons Attribution License, which permits unrestricted use, distribution, and reproduction in any medium, provided the original work is properly cited.

experiments by means of GCTS-type SWCC device for SWCC of remolded unsaturated loess specimen at different bulk densities under dry-wet cycle, and developed the concept named “degree of hysteresis” to study the SWCC hysteresis behavior of unsaturated loess. Zhao and Wang (2012) measured the SWCC of loess by Ku-pF apparatus and pressure plate extractors, as well as suggested the air entry value and residual water content. Also, the effects of dry density and dry-wet cycles on the SWCC of loess were analyzed through both experimental data and microstructure. Zhao et al. (2015) studied the effects of vertical stress and dry-wet cycles on SWCC of compacted unsaturated loess by using unsaturated soil oedometer. Liu and Ye (2015) studied the SWCC of unsaturated red clay by pressure plate instrument considering different influencing factors. Yang et al. (2016) used Tempe Membrane Gauge and Multifunctional SWCC Test Instrument to study the influences of drying-wetting cycle on SWCC of unsaturated clay considering consolidation pressure and compactness. Zhang et al. (2016) analyzed the effects of compactness and dry-wet cycles on the SWCC of silt soil in Eastern Henan, China. As far as permeability coefficient of unsaturated soil was concerned, Lian (2010; Lian et al., 2010) conducted penetration experiment of loess in Yangling Region of Shaanxi Province (in China) under the freeze-thaw cycles and confirmed that the freeze-thaw cycle had certain influence on the permeability and pore ratio of loess. Xiao et al. (2014) researched the effect of freeze-thaw on the permeability of loess. Liu et al. (2015) explored the SWCC under dry-wet cycles and predicted permeability coefficient of unsaturated loess.

In summary, most of the existing researches have focused on the effects of many impact factors such as water content, dry density, consolidation pressure, compactness and dry-wet cycles on SWCC. However, it is rarely noticed that the freeze-thaw action, coupling of freeze-thaw and dry-wet considering dry-wet path have effect on the matric suction of unsaturated loess. And the related research results on how the freeze-thaw cycle influences vertical distribution of unsaturated soil permeability coefficient have not been consulted. In view of the above analysis, this research has systematically studied how the freeze-thaw cycle, coupling of freeze-thaw and dry-wet action considering dry-wet path influence the matric suction and SWCC of unsaturated loess through laboratory experiments. At the same time, the Gardner Model, the Fredlund & Xing Model and the Van Genuchten Model were used to fit the SWCC under different experimental conditions, respectively. The applicability of each model was evaluated, and the Gardner Model was found to be more appropriate to describe the SWCC under the given

experimental conditions. As a result, according to measured SWCC from Gardner Model, the relationship between the unsaturated soil permeability coefficient and the matric suction or volumetric water content was established by using Childs & Collis-George Model. Using this relationship, the vertical distribution model of unsaturated soil permeability coefficient with the one-dimensional steady state flow under different freeze-thaw cycles was obtained. The research results may play a significant role in the investigation on SWCC and permeability coefficient prediction model for unsaturated loess considering freeze-thaw cycle or coupling of freeze-thaw and dry-wet action.

2. Experimental method

The soil samples used in the experiment are remolded loess. The loess is taken from a foundation pit engineering in the Qilihe District of Lanzhou City in China, and the soil is obtained from 5.0m to 6.0m under the ground surface. Representative soil is taken through quarter diagonal sampling method, and the grain composition of the soil obtained by the screening test is shown in Table 1.

The basic physical parameters of the loess used in the experiment are: liquid limit 25.8%, plastic limit 16.7%, plasticity index 9.1, maximum dry density 1.82g/cm³, optimum moisture content 15.6%, specific gravity of soil particles 2.72, saturated permeability coefficient 2.5×10⁻⁶ m/s. All the unsaturated remolded loess samples are obtained by manual compaction test, and soil material is passed through a 0.5mm standard sieve. The soil samples are prepared with water content of 10%, 12%, 14%, 16%, 18% and 20%, respectively. In order to make the water migrate evenly, the soil material is put into a sealed bag and sealed for 24 hours after mixing the soil evenly. The measured water content of soil samples are 9.75%, 11.45%, 13.60%, 15.85%, 17.57% and 19.33%, respectively. Dry density of all the prepared remolded samples is set as 1.60g/cm³, and the error is controlled within 0.05 g/cm³. The size of the soil samples is 2cm in height and 6cm in diameter.

This paper studies the effect of freeze-thaw action, coupling of freeze-thaw and dry-wet on SWCC of the unsaturated soil. Therefore, this research adopts an adjustable temperature refrigerator to simulate freeze-thaw cycle. In the test, the number of freeze-thaw cycles are set as 0, 1, 3, 5, 7 and 10 times, respectively. The prepared samples sealed with plastic wrap are put into the refrigerator and frozen for 12 hours (the temperature in the refrigerator is set as -17°C). After freezing, the samples are removed from the refrigerator and thawed at room temperature (17°C~20°C) for 12 hours to complete a whole freeze-thaw cycle. During

Table 1. Grain composition

Loess Soil	Particle size distribution (%)					
	>2mm	2~1mm	1~0.5mm	0.5~0.25mm	0.25~0.075mm	<0.075mm
Percent	9.5	4.8	10.7	11.4	31.9	31.7

the freezing-thawing process, the samples are in a closed state and no water is supplied from outside. In order to achieve the wetting and drying cycle, the natural air drying is used for dehydration and the titrated water injection is used for moisture absorption. There are two types of dry-wet paths. One of the dry-wet paths is first absorption and then desorption, which is named drying followed by wetting path. And another dry-wet path is first desorption and then absorption, which is called wetting followed by drying path. And the coupling times of freeze-thaw and dry-wet are set as 1, 2, 3 and 4 times respectively.

Under the above experimental conditions, the matric suction is measured by the filter paper method, which can be used to measure a large range of matric suction in the laboratory conveniently. According to the different contact degree between the filter paper and the soil, the filter paper method can be divided into direct contact method and non-contact method. The total suction of the soil is tested based on the non-contact method, and the direct contact method is used to measure matric suction. Herein, the contact method is adopted. The specific test steps are as follows. First, the filter papers are put into the oven and baked for 2 hours under temperature of 105°C, and then 3 pieces of baked filter paper are taken out with a tweezer. One filter paper is the measuring filter paper (diameter: 55mm), protected by the other two filter papers (diameter: 70mm). The measuring filter paper, weighed before and after each test by using an electronic balance (precision: 0.0001), is placed in the middle of the two protective filter papers, and the 3 pieces of filter paper are squeezed between two soil samples. The samples for measuring matric suction are sealed with adhesive tape and are placed in a sealed box for 7 days because the water between soil and filter paper will reach an equilibrium state after 7 days according to the related theory of unsaturated soil mechanics (Lu & Likos, 2012).

The Whatman’s No.42 ash-free quantitative filter paper is adopted, and Equation 1 and Equation 2 give the calibration curves between water content and matric suction of filter paper under equilibrium state, respectively:

$$\log s = 2.909 - 0.0229w_f, w_f \geq 47\% \tag{1}$$

$$\log s = 4.945 - 0.0673w_f, w_f < 47\% \tag{2}$$

where, s is matric suction (kPa); w_f is equilibrium water content of filter paper (%).

3. Experimental results and discussion

3.1 Effect of freeze-thaw cycle on matric suction

Freeze-thaw cycle, one of the typical weathering processes, has remarkable influence on the physical-mechanical behavior and hydraulic property of unsaturated soils. When the initial

dry density of remolded unsaturated loess is 1.60 g/cm³, the variation of the matric suction and its corresponding regression equation of soil samples with different water contents under freezing and thawing cycle are shown in Figure 1 and Table 2, respectively. Through the analysis of the experimental data, what can be seen from Figure 1 is that as the number of freeze-thaw cycle increases, the matric suction decreases gradually and tends to stabilize. As regards the soil samples with different water contents, the change of matric suction is the largest when freeze-thaw occurs once, and the variation amplitude of matric suction gradually decreases with the number of freeze-thaw cycle continuing to increase. After 7 freeze-thaw cycles, the matric suction basically tends to be stable. This happens mainly because the freeze-thaw action causes the ice crystals in the pores to expand, which makes the arrangement and connection of soil particles be changed and the initial soil structure be destroyed, and results in pores development and fissures formation. The fissures are generated among the soil particles, which leads to the adhesion of soil particles decreases and the water film among the soil particles disintegrates, so the matric suction in the soil decreases. As the number of freeze-thaw cycle continues to increase, the original structure is gradually damaged and a new relatively stable structure is slowly formed. Therefore, after 7 freeze-thaw cycles, the effect of freeze-thaw on the matric suction tends to be stable. It can be seen from Table 2 that the changing process of matric suction with the number

Table 2. Regression equation of matric suction and freeze-thaw cycles

Water content (%)	Regression equation	R ²
9.75	$y=209.313-49.119\ln(x+0.037)$	0.9747
11.45	$y=54.364-4.426\ln(x+0.003)$	0.9196
13.60	$y=43.728-4.333\ln(x+0.181)$	0.9062
15.85	$y=35.791-4.394\ln(x+0.109)$	0.8710
17.57	$y=17.834-1.832\ln(x+0.007)$	0.9141
19.33	$y=8.351-3.222\ln(x+0.082)$	0.8599

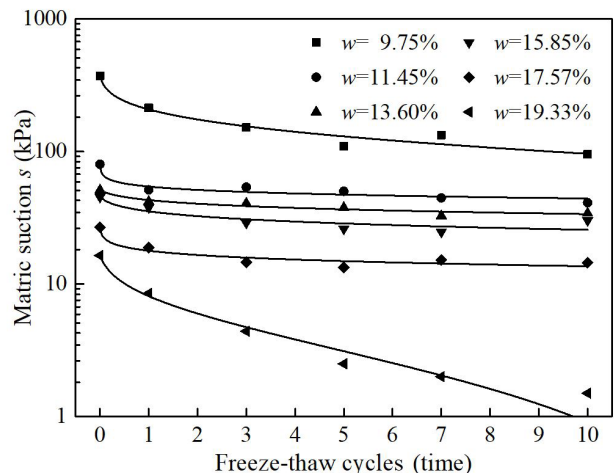


Figure 1. The relation between matric suction and freeze-thaw cycles.

of freeze-thaw cycles follows logarithmic curve and the correlation coefficient reaches significant level.

3.2 Effect of coupling of freeze-thaw and dry-wet on matric suction

In northwestern China, the climate experiences dry-wet alternation and freeze-thaw cycle repeatedly, and this has a significant influence on the mechanical behavior of shallow unsaturated soil. According to the previous research results, various dry-wet paths have obvious effect on the matric suction of unsaturated soil. Under the same water content, the matric suction under drying followed by wetting path would be greater than that under wetting followed by drying, which indicates that different dry-wet paths lead to different strengths of unsaturated soil. The variation of the matric suction and its corresponding regression equation of soil samples under coupling of freeze-thaw and dry-wet considering different dry-wet paths are shown in Figure 2 and Table 3, respectively.

It can be seen from Figure 2 that when studying the effect of the coupling of freeze-thaw and dry-wet on the

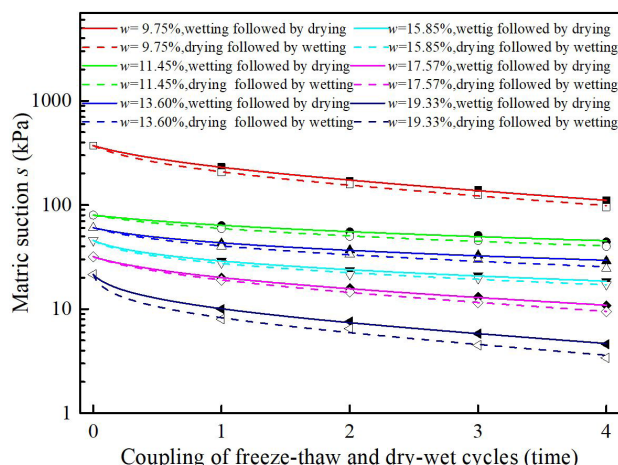


Figure 2. The relation between matric suction and coupling of freeze-thaw and dry-wet.

Table 3. Regression equation of matric suction and freeze-thaw/dry-wet cycles

Dry-wet path	Water content (%)	Regression equation	R ²
wetting followed by drying	9.75	$y=222.557-86.674\ln(x+0.179)$	0.9083
	11.45	$y=65.194-16.705\ln(x+0.412)$	0.9013
	13.60	$y=43.056-12.144\ln(x+0.238)$	0.9228
	15.85	$y=28.246-7.881\ln(x+0.110)$	0.9059
	17.57	$y=20.747-7.787\ln(x+0.242)$	0.9157
	19.33	$y=8.336-3.397\ln(x+0.021)$	0.9012
drying followed by wetting	9.75	$y=258.952-101.156\ln(x+0.328)$	0.9089
	11.45	$y=73.638-18.295\ln(x+0.709)$	0.8981
	13.60	$y=46.268-11.554\ln(x+0.292)$	0.9267
	15.85	$y=30.039-8.056\ln(x+0.145)$	0.9159
	17.57	$y=21.905-7.577\ln(x+0.271)$	0.9078
	19.33	$y=10.343-4.043\ln(x+0.063)$	0.9095

matrix suction, different dry-wet action paths similarly have a certain influence on the matric suction of the unsaturated remolded loess. In general, for the soil samples with the same water content, the matric suction under the path of drying followed by wetting is slightly larger than that under the path of wetting followed by drying. When the coupling of freeze-thaw and dry-wet is once, the change of matric suction is the largest, and the variation amplitude becomes smaller and tends to stabilize with the increase of coupling number. This conclusion is consistent with the research results of the literature (Qi et al., 2005), which pointed the first freeze-thaw cycle had the greatest influence on soil properties and there was little effect on soil after 3-5 freeze-thaw cycles. And the matric suction changing with the coupling of freeze-thaw and dry-wet cycle follows logarithmic curve and the correlation coefficient reaches a significant level (Table 3).

3.3 SWCC curve fitting

3.3.1 SWCC fitting model

In order to attain unsaturated soil permeability coefficient model from limited experimental data or predict the permeability coefficient equation from conventional constitutive equations especially SWCC model, researchers have developed many mathematical models. Three kinds of SWCC models, including Gardner equation, Fredlund & Xing equation and Van Genuchten equation, commonly used in geotechnical engineering are introduced to predict the permeability coefficient equation.

1. Gardner equation

$$\theta_w = \theta_r + \frac{\theta_s - \theta_r}{1 + \left(\frac{\psi}{a}\right)^b} \tag{3}$$

where, θ_w is volumetric water content (%); θ_s and θ_r are the saturated and residual volumetric water content (%), respectively; ψ is the matric suction (kPa); a is a parameter related to the air entry value (kPa); b is a parameter related to the soil dehydration rate when the matric suction is larger than the air entry value.

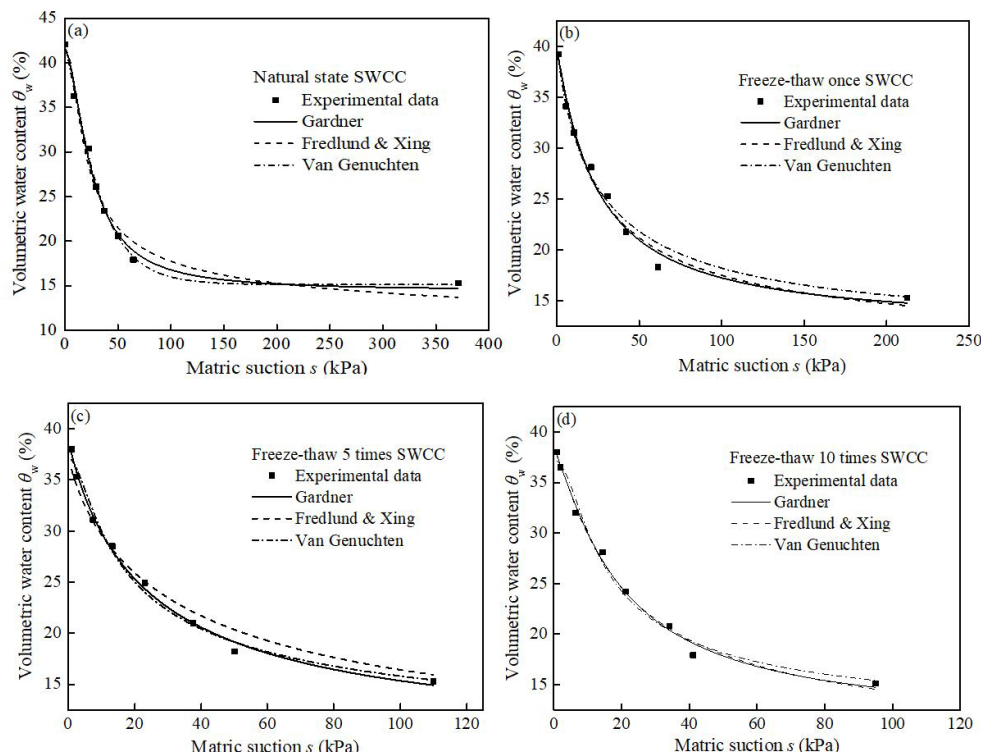


Figure 3. Function fitting for SWCC of different freeze-thaw cycles: (a) Natural state; (b) Freeze-thaw once; (c) Freeze-thaw 5 times; (d) Freeze-thaw 10 times.

2. Fredlund & Xing equation

$$\theta_w = \frac{\theta_s}{\left\{ \ln \left[e + \left(\frac{\psi}{a} \right)^b \right] \right\}^c} \quad (4)$$

where, c is a parameter related to residual water content; $c=2.71828$, and the other letters represent the same meanings as Formula 3.

3. Van Genuchten equation

$$\theta_w = \theta_r + \frac{\theta_s - \theta_r}{\left[1 + (a \cdot \psi)^b \right]^c} \quad (5)$$

where, the letters represent the same meanings as Formula 3 and Formula 4, respectively.

3.3.2 SWCC model fitting under freeze-thaw action

The Gardner Model, the Fredlund & Xing Model and the Van Genuchten Model are used to fit the measured matric suction under different freeze-thaw cycles, respectively. The experimental data and fitting curve are shown in Figure 3. The fitting parameters of each model equation under different freeze-thaw cycles are shown in Table 4, respectively. Due to space constraints, the experimental results of freeze-thaw for 0, 1, 5, and 10 times are only highlighted because there are generally similar rules under other freeze-thaw cycles.

In general, the fitting effect of the Gardner Model is the best. The Van Genuchten Model has the second fitting effect, and the Fredlund & Xing Model has a slightly worse fitting effect.

3.3.3 SWCC function fitting under coupling of freeze-thaw and dry-wet cycle

In the same way, these three typical theoretical models including Gardner Model, Fredlund & Xing Model and Van Genuchten Model are used to fit the experimental data under coupling of freeze-thaw cycle and dry-wet alternation considering dry-wet paths, respectively. The fitting results are shown in Figure 4 and the fitting parameters of each model equation are shown in Table 5, respectively. Similarly, in order to save space, the experimental results of freeze-thaw and dry-wet coupling for 1, 4 times are listed in Table 5. Through comparative analysis, the fitting effect of the Gardner Model is the best. The Van Genuchten Model has the second fitting effect, and the Fredlund & Xing Model has a slightly worse fitting effect, too.

3.4 Prediction of unsaturated permeability coefficient

According to the above fitting rules of SWCC under different experimental conditions, it is concluded that the experimental data are fitted by using Gardner Model, which has the best fitting effect. Therefore, the experimental SWCC is obtained in line with the Gardner Model fitting. The permeability coefficient of unsaturated soil is not constant, and it is a function of matric suction. With the use of permeability

Table 4. The fitting values of parameters

Engineering conditions	Model types	<i>a</i>	<i>b</i>	<i>c</i>	θ_r	θ_s	R^2
Natural state	Gardner	25.062	1.700		14.442	41.416	0.9329
	Fredlund & Xing	10.852	2.035	0.562		41.576	0.9101
	Van Genuchten	0.005	1.240	10.215	15.127	41.772	0.9404
Freeze-thaw once	Gardner	24.345	1.080		12.389	39.585	0.9300
	Fredlund & Xing	9.656	1.149	0.781		39.688	0.9255
	Van Genuchten	0.034	0.826	1.120	11.518	40.836	0.9101
Freeze-thaw 5 times	Gardner	24.202	0.9189		8.888	39.140	0.9422
	Fredlund & Xing	16.379	0.844	1.199		37.488	0.9085
	Van Genuchten	0.146	1.834	0.238	6.183	37.195	0.9276
Freeze-thaw 10 times	Gardner	19.596	1.210		11.231	38.338	0.9391
	Fredlund & Xing	9.443	1.266	0.867		38.348	0.9373
	Van Genuchten	0.129	2.182	0.295	9.999	37.191	0.9219

Table 5. The fitting values of parameters

Dry-wet path	Engineering conditions	Model types	<i>a</i>	<i>b</i>	<i>c</i>	θ_r	θ_s	R^2
Absorption before desorption	Coupling once	Gardner	22.641	1.087		12.671	39.770	0.9330
		Fredlund & Xing	5.167	0.823	0.813		41.034	0.8864
		Van Genuchten	0.004	0.893	7.234	14.673	40.134	0.9152
	Coupling 4 times	Gardner	17.512	0.919		10.362	39.126	0.9365
		Fredlund & Xing	5.937	1.001	0.882		38.981	0.9263
		Van Genuchten	0.082	1.200	0.677	9.145	36.598	0.8791
Desorption before absorption	Coupling once	Gardner	22.421	1.297		13.290	40.189	0.9380
		Fredlund & Xing	9.550	1.143	0.814		40.869	0.9282
		Van Genuchten	0.049	0.961	0.831	11.803	41.698	0.8695
	Coupling 4 times	Gardner	14.567	1.137		11.795	40.353	0.9416
		Fredlund & Xing	6.194	1.026	0.995		41.051	0.9275
		Van Genuchten	22.421	1.297		13.290	40.189	0.9380

coefficient on Childs & Collis-George Model, the relationship between permeability coefficient and matric suction is built on the experimental SWCC. The SWCC is divided into m equal parts along the volumetric water-content axis, and the unsaturated permeability coefficient $k(\theta)_i$ is calculated by using the matric suction of each equal part's midpoint according to the following formula.

$$k(\theta)_i = \frac{k_s}{k_{sc}} A_d \sum_{j=i}^m \left[(2j+1-2i)(u_a - u_w)_j^{-2} \right] \quad (6)$$

$i = 1, 2, \dots, m$

where, $k(\theta)_i$ is permeability coefficient determined by volumetric water content (θ)_{*i*} corresponding to the midpoint of *i*-th segment (m/s); k_s is the measured saturated permeability coefficient (m/s), and it is 2.5×10^{-6} m/s; k_{sc} is the calculated saturated permeability coefficient (m/s); A_d is the adjustment constant ($m \cdot s^{-1} \cdot kPa^2$); *i* is segment number; *j* is a number from *i* to *m*; *m* is the total number of segments from the saturated volumetric water content θ_s to the lowest volumetric water content θ_L on the soil-water characteristic curve (That is, $m=20$); $(u_a - u_w)_j$ is matric suction value corresponding to the midpoint of the *j*-th segment (kPa); And A_d is obtained by Formula 7.

$$A_d = \frac{T_s^2 \rho_w g \theta_s^p}{2\mu_w N^2} \quad (7)$$

where, T_s is the surface tension of water (kN/m); ρ_w is the density of water (kg/m³); *g* is the acceleration of gravity (m/s²); μ_w is the absolute viscosity of water (N·s/m²); θ_s is the saturated volumetric water content (%); *p* is the constant considering the interaction between pores of different sizes, set as 2.0 (Green & Corey); *N* is the total number of segments between saturated volumetric water content and zero volumetric water content ($\theta_w = 0$), $N = m[\theta_s / (\theta_s - \theta_L)]$, $m \leq N$.

And k_{sc} in Formula 6 is obtained from Formula 8.

$$k_{sc} = A_d \sum_{j=i}^m \left[(2j+1-2i)(u_a - u_w)_j^{-2} \right] \quad (8)$$

$$i = 0, 1, 2, \dots, m$$

where, $(u_a - u_w)_j$ is the matric suction value corresponding to the midpoint of the *j*-th segment (kPa); the other letters represent the same meanings as Formula 6 and Formula 7, respectively.

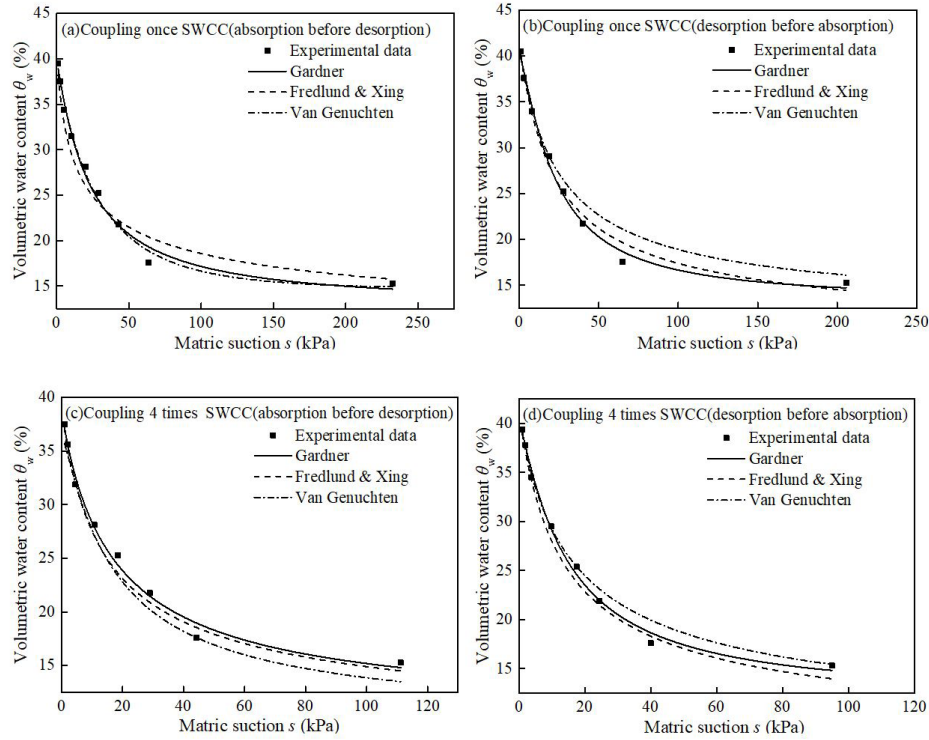


Figure 4. Function fitting for SWCC of different coupling of freeze-thaw and dry-wet: (a) Coupling once and absorption before desorption; (b) Coupling once and desorption before absorption; (c) Coupling 4 times and absorption before desorption; (d) Coupling 4 times and desorption before absorption.

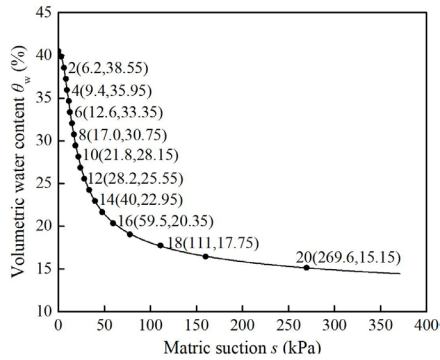


Figure 5. The predicting method of permeability coefficients based on soil-water characteristic curve.

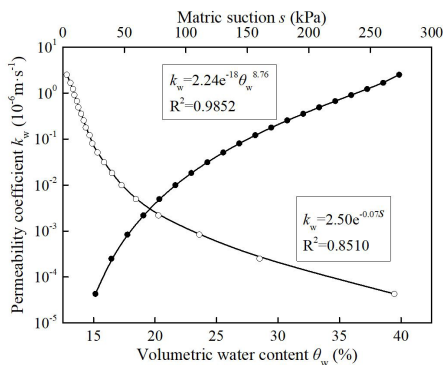


Figure 6. The permeability coefficient function.

The SWCC fitted based on the Gardner Model according to the experiment data is shown in Figure 5. When the experimental temperature is 20°C, the surface tension of water is that $T_s = 7.28 \times 10^{-5} \text{ kN/m}$; absolute viscosity of water is that $\mu_w = 100.5 \times 10^{-5} \text{ N} \cdot \text{s} \cdot \text{m}^{-2}$; and the minimum volumetric water content on the SWCC obtained from the experiment is that $\theta_L = 14.5\%$; by calculating, $N = 32$, $A_d = 4.14 \times 10^{-2} \text{ m} \cdot \text{s}^{-1} \cdot \text{kPa}^2$, $k_{sc} = 3.31 \times 10^{-2} \text{ m} \cdot \text{s}^{-1}$, $k_s / k_{sc} = 7.55 \times 10^{-5}$, respectively, which are used to calculate all unsaturated permeability coefficient subsequently. The permeability coefficients calculated by the matric suction at the midpoint of each equal part are shown in Table 6.

Based on the above analysis, the changes of permeability coefficient with matric suction and volumetric water content are given in Figure 6, respectively. It can be seen that the relationship between the permeability coefficient and the matric suction can be expressed by an exponential function, and the permeability coefficient decreases sharply with the matric suction increases. And the relationship between the permeability coefficient and the volumetric water content can be expressed in the form of a power function formula.

The regression equations between the unsaturated permeability coefficient and the matric suction as well as the volumetric water content are expressed by Formula 9 and Formula 10, respectively.

$$k_w = (2.50 \times 10^{-6}) e^{-0.075s} \tag{9}$$

Table 6. The calculated permeability coefficients under different matric suctions

Interval i	Volumetric water contents (θ_i) (%)	Matric suctions $u_a - u_w$ (kPa)	Permeability coefficients $k(\theta)_i$ (m/s)
1	39.85	3.2	2.500×10^{-6}
2	38.55	6.2	1.669×10^{-6}
3	37.25	8.3	1.224×10^{-6}
4	35.95	9.4	9.063×10^{-7}
5	34.65	11.5	6.690×10^{-7}
6	33.35	12.6	4.906×10^{-7}
7	32.05	14.9	3.532×10^{-7}
8	30.75	17.0	2.543×10^{-7}
9	29.45	18.7	1.779×10^{-7}
10	28.15	21.8	1.213×10^{-7}
11	26.85	24.0	8.017×10^{-8}
12	25.55	28.2	5.107×10^{-8}
13	24.25	33.6	3.132×10^{-8}
14	22.95	40	1.827×10^{-8}
15	21.65	47.8	9.946×10^{-9}
16	20.35	59.5	4.942×10^{-9}
17	19.05	77.8	2.189×10^{-9}
18	17.75	111	8.350×10^{-10}
19	16.45	160	2.511×10^{-10}
20	15.15	269.6	4.300×10^{-11}

where, k_w is the unsaturated permeability coefficient ($m \cdot s^{-1}$); s is the matric suction (kPa).

$$k_w = (2.24 \times 10^{-6}) e^{-1.8 \theta_w^{8.76}} \quad (10)$$

where, k_w is the unsaturated permeability coefficient ($m \cdot s^{-1}$); θ_w is the volumetric water content (%).

3.5 Vertical distribution model of permeability coefficient of one-dimensional steady flow unsaturated soil

Due to the vertical joints and pore development of loess, the permeability coefficient of loess is anisotropic and the vertical permeability coefficient is significantly larger than the horizontal permeability coefficient. Therefore, for the construction of the loess engineering, it is of great significance to study the vertical permeability coefficient of unsaturated loess. It is known that the vertical unsaturated flow can be expressed by Darcy's Law under steady state. The water flow flowing downward is set as negative sign and flowing upward is set as positive sign, and the specific discharge expression in the vertical direction is by Formula 11.

$$q = -k_w \left[\frac{d(u_w - u_a)}{\gamma_w dy} + 1 \right] \quad (11)$$

where, q is specific discharge ($m \cdot s^{-1}$); γ_w is the bulk density of water (kN / m^3); y is the position from water table in vertical direction (m); the other letters represent the same meanings as above, respectively.

The water table is set as $y = 0$, and y above the water table is positive. By boundary condition that when $y = 0$, the matric suction is 0, and the distribution model of the matric suction along the direction y is derived from the Formula 9 and Formula 11 as follows:

$$0.07s = -\ln \left[\left(1 + \frac{q}{2.50 \times 10^{-6}} \right) e^{-0.07 \gamma_w y} - \frac{q}{2.50 \times 10^{-6}} \right] \quad (12)$$

where, the letters represent the same meanings as above, respectively.

By substituting Equation 12 into Equation 9, the expression of one-dimensional steady state unsaturated permeability coefficient distributed vertically in the natural engineering condition is derived as Formula 13.

$$k_y = (2.50 \times 10^{-6}) e^{\ln \left[\left(1 + \frac{q}{2.50 \times 10^{-6}} \right) e^{-0.07 \gamma_w y} - \frac{q}{2.50 \times 10^{-6}} \right]} \quad (13)$$

$$= (2.50 \times 10^{-6}) \left[\left(1 + \frac{q}{2.50 \times 10^{-6}} \right) e^{-0.07 \gamma_w y} - \frac{q}{2.50 \times 10^{-6}} \right]$$

where, k_y is vertical permeability coefficient ($m \cdot s^{-1}$); the other letters represent the same meanings as above, respectively.

Similarly, the expression of one-dimensional steady state unsaturated permeability coefficient distributed vertically under the experimental condition of one freeze-thaw cycle is derived as Formula 14.

$$k_y = (1.69 \times 10^{-6}) \left[\left(1 + \frac{q}{1.69 \times 10^{-6}} \right) e^{-0.1 \gamma_w y} - \frac{q}{1.69 \times 10^{-6}} \right] \quad (14)$$

where, the letters represent the same meanings as above, respectively.

The expression of one-dimensional steady state unsaturated permeability coefficient distributed vertically under the experimental condition of 10 freeze-thaw cycles is derived as Formula 15.

$$k_y = (3.24 \times 10^{-6}) \left[\left(1 + \frac{q}{3.24 \times 10^{-6}} \right) e^{-0.03\gamma_w \cdot y} - \frac{q}{3.24 \times 10^{-6}} \right] \quad (15)$$

where, the letters represent the same meanings as above, respectively.

By using the vertical distribution models of unsaturated permeability coefficient under the above different experimental conditions to calculate and analyze, the results are shown in Figure 7. The calculating soil layer is homogeneous soil layer with a thickness of 10m, water table $y = 0m$, the earth's surface $y = 10m$, specific discharge $q = -3.14 \times 10^{-8} m \cdot s^{-1}$.

As can be seen from Figure 7, the permeability coefficients distributed vertically of unsaturated loess under different freeze-thaw cycles have the same trend as that in the natural condition. That is, the permeability coefficient from the water table to the ground surface shows a decreasing trend. After undergoing the freeze-thaw action, the vertical permeability coefficient of the soil has been reduced by 1 or 2 orders of magnitude. The vertical permeability coefficient at the same depth of soil layer shows the law of decreasing first, then increasing and tending to be stable with the number of freeze-thaw increasing. Mainly because the loess has the features of vertical joint developing, large pores, loose structure and weak cementation, when the water in the soil freezes to form the ice crystals and the soil volume expands, there is enough pore space among the particles caused by frost heave and the soil structure will be strongly damaged. At the same time, the ice crystals formed during the freezing process have a pressure effect on the soil particles, which makes the particles to compact with each other, so the void ratio decreases and accordingly the permeability coefficient

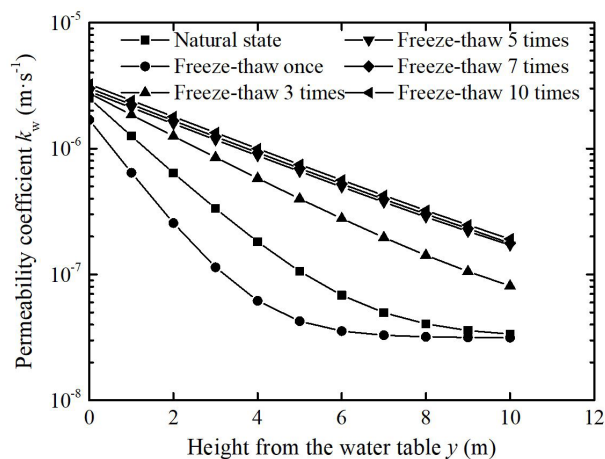


Figure 7. The calculation of vertical permeability coefficient under different conditions.

increases. For unsaturated soil, the pore water exists as adsorbed water films on the soil particles, so a smaller void ratio results in a greater permeability coefficient under the same matric suction. With the continuous increase of the number of freeze-thaw, the effect of freeze-thaw action on soil particles and structures becomes weakened and the void ratio tends to be stable, which makes the permeability coefficient tend to be stable.

4. Conclusions

As the typical weathering processes, freeze-thaw action and dry-wet alternation both have significant impacts on the structure of soil, thus changing its physical and mechanical properties. In this study, based on filter paper method, the SWCC on unsaturated loess considering freeze-thaw cycle, coupling of freeze-thaw cycle and dry-wet action was carried out, and some valuable conclusions were drawn according to the experimental data.

4. The first freeze-thaw cycle has the greatest influence on matric suction. As the number of freeze-thaw cycle increases, the matric suction decreases gradually and basically tends to be stable after 7 freeze-thaw cycles. Under the same water content, the matric suction with the number of freeze-thaw cycles follows logarithmic curve;
5. The first coupling of freeze-thaw and dry-wet action has the greatest influence on matric suction. With the increase of coupling times, the matric suction of unsaturated loess was logarithmically decreasing, and the dry-wet path affected matric suction significantly. For the soil samples with the same water content, the matric suction under the path of drying followed by wetting is slightly larger than that under the path of wetting followed by drying;
6. For Gardner Model, Fredlund & Xing Model and Van Genuchten Model, the Gardner Model is more appropriate to describe the SWCC under given experimental conditions, so according to measured SWCC from Gardner Model and by using Childs & Collis-George Model, the prediction model of unsaturated loess permeability coefficient is gained, and the permeability coefficient has an exponential relationship with matric suction and a power function relationship with volumetric water content, respectively;
7. The vertical permeability coefficient of unsaturated loess decreases from groundwater level to surface under different freeze-thaw cycles. At the same depth of soil, it decreases and then increase and gradually stabilize with the increase of freeze-thaw cycles.

Acknowledgements

This research project was funded by the National Natural Science Foundation of China (Grant No. 51769013, 41971093) and Basic Research Innovation Group of Gansu (20JR5RA478).

Declaration of interest

The authors declare that there are no conflicts of interest regarding the publication of this paper.

Author's contributions

Yaling Chou: idea, conceptualization, methodology, validation, writing - reviewing and editing, language. Lijie Wang: experiment, data curation, writing - original draft preparation, investigation, modeling, validation.

References

- Bai, F.Q., Liu, S.H., & Yuan, J. (2011). Measurement of SWCC of Nanyang expansive soil using the filter paper method. *Chinese Journal of Geotechnical Engineering*, 33(6), 928-933.
- Bishop, A.W., Alpan, I., Blight, G.E., & Donald, I.B. (1960). Factors controlling the strength of partly saturated cohesive soils. In *Proceedings of the A.S.C.E. Conference on the Shear Strength of Cohesive Soils* (pp. 503-532). New York: ASCE.
- Chen, Z.H. (1999). Deformation, strength, yield and moisture change of a remolded unsaturated loess. *Chinese Journal of Geotechnical Engineering*, 21(1), 82-90. <http://dx.doi.org/10.3321/j.issn:1000-4548.1999.01.018>.
- Fredlund, D.G., Xing, A.Q., & Huang, S.Y. (1994). Predicting the permeability function for unsaturated soils using the soil-water characteristic curve. *Canadian Geotechnical Journal*, 31(4), 533-546. <http://dx.doi.org/10.1139/t94-062>.
- Fredlund, D.G., & Rahardjo, H. (1997). *Soil mechanics for unsaturated soils*. Beijing: China Architecture and Building Press.
- Fredlund, D.G., Xing, A.Q., Fredlund, M.D., & Barbour, S.L. (1996). The relationship of the unsaturated soil shear strength to the soil-water characteristic curve. *Canadian Geotechnical Journal*, 33(3), 440-448. <http://dx.doi.org/10.1139/t96-065>.
- Li, Z.Q., Li, T., Hu, R.L., Li, X., & Li, Z.J. (2007). Methods for testing and predicting of SWCC in unsaturated soil mechanics. *Journal of Engineering Geology*, 15(5), 700-707. <http://dx.doi.org/10.3969/j.issn.1004-9665.2007.05.020>.
- Lian, J.B. (2010). *Study on the variation of physical properties of loess under freezing-thawing cycles*. Northwest A & F University, Yangling, shaanxi, China.
- Lian, J.B., Zhang, A.J., Guo, M.X., & Dong, X.H. (2010). Influence of iterative freezing-thawing on void ratio and permeability coefficient of loess. *Yangtze River*, 41(12), 55-58.
- Liu, F.Y., Zhang, Z., Zhou, D., Zhao, X.G., & Zhu, L. (2011). Effects of initial density and drying-wetting cycle on soil water characteristic curve of unsaturated loess. *Rock and Soil Mechanics*, 33(S2), 132-136+142. <https://doi.org/10.16285/j.rsm.2011.s2.086>.
- Liu, P.F., Yin, Y.P., Li, B., & Sun, Y.B. (2015). The tests of soil-water characteristic curve and permeability coefficient prediction of the wetting-drying cycles for unsaturated loess. *The Chinese Journal of Geological Hazard and Control*, 26(4), 125-129. <http://dx.doi.org/10.16031/j.cnki.issn.1003-8035.2015.04.22>.
- Liu, X.W., & Ye, Y.X. (2015). Experimental study of the soil-water characteristic curve of unsaturated laterite under different affecting factors. *Hydrogeology & Engineering Geology*, 59(2), 97-104. <http://dx.doi.org/10.16030/j.cnki.issn.1000-3665.2015.02.15>.
- Liu, Z., Zhang, B., Yu, X., & Tao, J.L. (2012). A new method for soil water characteristic curve measurement based on similarities between soil freezing and drying. *Geotechnical Testing Journal*, 35(1), 2-10. <http://dx.doi.org/10.1520/GTJ103653>.
- Lu, J., & Cheng, B. (2007). Research on soil-water characteristic curve of unsaturated loess. *Chinese Journal of Geotechnical Engineering*, 29(10), 1591-1592. <http://dx.doi.org/10.3321/j.issn:1000-4548.2007.10.027>.
- Lu, N., & Likos, W.J. (2012). *Unsaturated soil mechanics*. Beijing: China Higher Education Press.
- Qi, J.L., Cheng, G.D., & Vermeer, P.A. (2005). State-of-the-art of influence of freeze-thaw on engineering properties of soils. *Diqiu Kexue Jinzhan*, 20(8), 887-894. <http://dx.doi.org/10.3321/j.issn:1001-8166.2005.08.010>.
- Sillers, W.S., Fredlund, D.G., & Zakerzadeh, N. (2001). Mathematical attributes of some soil-water characteristic curve models. *Geotechnical and Geological Engineering*, 19(3), 243-283. http://dx.doi.org/10.1007/978-94-015-9775-3_3.
- Vanapalli, S.K., Fredlund, D.G., & Pufahl, D.E. (1996). The relationship between the soil-water characteristic curve and unsaturated shear strength of a compacted glacial till. *Geotechnical Testing Journal*, 19(3), 259-268. <http://dx.doi.org/10.1520/gtj10351j>.
- Wang, Z., Yang, J.X., Kuang, J.J., An, J.Y., & Luo, Y.D. (2003). Application of filter paper method in field measurement of matric suction. *Chinese Journal of Geotechnical Engineering*, 25(4), 405-408. <http://dx.doi.org/10.3321/j.issn:1000-4548.2003.04.004>.
- Xiao, D.H., Feng, W.J., Zhang, Z., Ming, J., & Wang, Q. (2014). Research on the Lanzhou loess's permeabilities changing with freezing-thawing cycles. *Journal of Glaciology and Geocryology*, 36(5), 1192-1198. <http://dx.doi.org/10.7522/j.issn.1000-0240.2014.0142>.
- Xiong, C.R., Liu, B.C., & Zhang, J.S. (2005). Relation of matric suction with moisture state and density state of remolded cohesive soil. *Chinese Journal of Rock Mechanics and Engineering*, 24(2), 321-327. <http://dx.doi.org/10.3321/j.issn:1000-6915.2005.02.023>.
- Yang, Y., Chen, Y., Li, P., & Tang, J.X. (2016). Influence of compaction and drying-wetting cycle with loading on soil-water characteristic curve. *Water Resources and Power*, 34(3), 128-131.
- Zhang, T., Yue, J.C., & Zhang, J.R. (2016). Influence of compaction degree and drying-wetting cycle on the soil water characteristic curve of Yudong silt. *Journal*

- of Zhengzhou University*, 37(6), 53-57. <http://dx.doi.org/10.13705/j.issn.1671-6833.2016.03.027>.
- Zhao, T.Y., & Wang, J.F. (2012). Soil-water characteristic curve for unsaturated loess soil considering density and wetting-drying cycle effects. *Journal of Central South University*, 57(6), 2445-2453.
- Zhao, W.B., Xu, J., Cheng, Q., & Lu, Y.H. (2015). Influences of vertical stress and drying-wetting cycles on soil-water characteristic curve of loess. *Kexue Jishu Yu Gongcheng*, 15(36), 189-193. <http://dx.doi.org/10.3969/j.issn.1671-1815.2015.36.034>.